이학석사학위논문

Atmospheric Circulation and Precipitation Fields over the tropical Indo-Pacific Region Associated with the Biennial Oscillation of Sea Surface Temperature

해수면 온도의 격년 진동과 관계된
열대 인도-태평양 지역에서의 대기 순환장 및 강수장

2015 년 8 월

서울대학교 대학원

지구환경과학부

김 진 주

Atmospheric Circulation and Precipitation Fields over the tropical Indo-Pacific Region Associated with the Biennial Oscillation of Sea Surface Temperature

지도교수 **Kwang-Yul Kim**

이 논문을 이학석사학위논문으로 제출함

2015년 6월

서울대학교 대학원

지구환경과학부

김 진 주

김진주 의 석사학위논문을 인준함

2015년 7월

위 원 장 손석우 (인)

부위원장 김 광 열 (인)

위 원 전 종 갑 (인)

Abstract

Atmospheric Circulation and Precipitation Fields over the tropical Indo-Pacific Region Associated with the Biennial Oscillation of Sea Surface Temperature

Jinju Kim

School of Earth and Environmental Sciences

The Graduate School

Seoul National University

Temporal and spatial patterns of atmospheric circulation and precipitation over Indo-Pacific region are analyzed in conjunction with the biennial mode of sea surface temperature anomalies (SSTA). It is investigated how the biennial mode modifies the Asian-Australian monsoon precipitation, which features the seasonal migration of precipitation band. In an attempt to document the impact of the biennial mode on the Asia-Australian monsoon precipitation, two-year cycle variability of SSTA and key atmospheric variables is separated from the seasonal cycle via Cyclostationary EOF (CSEOF) analysis. The monthly Extended Reconstruction SST version 3 (ERSST v.3) and the twentieth century reanalysis version 2 (20CR) are used. The biennial evolution of atmospheric variables is clearly seen over the tropical Indo-Pacific region (90°-150°E, 20°S-20°N). In boreal summer, local meridional circulation is a distinguishing characteristic over

the tropical Indo-Pacific region, whereas a north-south expanded branch of an intensified zonal circulation develops in austral summer. In boreal summer, low-level anticylonic/cyclonic circulation over the western North Pacific is linked with the northern branch of the local meridional circulation. Essential factors responsible for the distinctive atmospheric responses in the two seasons are the intensity and size of SSTA over the central-eastern Pacific and the different timings of the phase transition in the tropical Pacific and the Indian Ocean. The impact of the biennial mode is clearly different between the two seasons with substantially different impact on the Asian monsoon and the Australian monsoon.

Keywords: biennial variability, sea surface temperature, CSEOF analysis, atmospheric circulation, Asian-Australian monsoon precipitation, seasonal difference, the tropical Indo-Pacific

Student number: 2013-22971

Contents

List of Figures

1. Introduction

Bulk of tropical SSTA variability can be explained in terms of low-frequency variability associated with the Northern Pacific decadal oscillations, (quasi) biennial variability (Barnett 1991; Rasmusson et al. 1990; Kim 2002; Clarke et al. 1998) and global warming (Yeo and Kim 2014). Yeo and Kim (2014) showed that the sum of these three modes averaged over the Niño3 or Niño4 regions is highly correlated with the respective Niño index, and a significant part of tropical SST variability including the ENSO events is explained as the interplay of these nearly independent physical characteristics. Each of the three modes is associated with ENSO, but they represent distinct physical processes. Among them, the role played by the quasi-biennial variability, a prominent feature in the tropical Indian and Pacific Oceans, is a crucial element for understanding the mechanism of tropospheric biennial oscillation (TBO) (Meehl et al. 2003). There were many studies expounding the structure and mechanism of this ocean-atmospheric coupled phenomenon, which involves changes in pressure, precipitation, SST and wind, affecting various local monsoons over the Indo-Pacific region. Meehl (1987), Meehl and Arblaster (2002) and Meehl et al. (2003) reported that the southeastward migration of the convection center associated with the Indian-Australian monsoon ties the Pacific and Indian Oceans and is a main factor for the system's two-year fluctuation. Shen and Lau (1995) viewed that the anomalous wind over the western Pacific associated with the inherent biennial tendency in the tropical central/eastern SSTA is central to the biennial oscillation in the East Asian

monsoon. Wang et al. (2000, 2001) and Liu et al. (2013) elaborated that the biennial tendency in the tropical Pacific induces anomalous cyclone/anticyclone over the western North Pacific, thereby modulating the East Asian summer monsoon. On the other hand, it was also suggested that local SSTA over the Indo-Pacific warm pool interacting with the western North Pacific Subtropical High could produce 2-3 year variability (Chang and Li 2000; Chung et al. 2011; Li et al. 2006).

This biennial variability of the large-scale coupled system in the tropics can influence the interannual variability of the global monsoon system. The global monsoon represents the global-scale seasonal variation of the three-dimensional atmospheric circulation and corresponding precipitation change (Wang et al. 2014; An et al. 2014; Trenberth et al. 2000). Thus it is crucial to understand the Earth's climate system in association with the transport of atmospheric energy and water vapor (Wang 2009; An et al. 2015). Over the Indo-Pacific region, in particular, complicated change occurs in accordance with a large seasonal fluctuation. Also change in the monsoon rainfall exerts considerable societal and economical impact to many adjacent countries. Therefore, a rigorous investigation of the biennial process together with its impact is necessary for more accurate climate forecasts.

In many previous studies, biennial variability is explained in the presence of strong seasonal variability. However, it is necessary to separate the biennial mode from the seasonal cycle for a precise interpretation of the intrinsic evolution feature and physical mechanism of the biennial mode in time and space. Changes in local precipitations as stationary monsoon systems have been studied frequently

over East Asia and the western North Pacific (Shen and Lau 1995; Li et al. 2006; Chung et al. 2011; Liu et al. 2013; Li et al. 2013; Liu et al. 2014) and South Asia and India (Pillai and Mohankumar 2008; Wu and Kirtman 2004a). Study of monsoon precipitations as seasonally migrating systems, e.g., the Indian-Australian linked monsoon system, is relatively few (Chang and Li 2000; Meehl 1997; Meehl and Arblaster 2002; Webster et al. 1998). Further, not much attention was given to the difference in the atmospheric response and interaction between the transition and development stage of SSTA in boreal spring/summer and the mature stage of SSTA in boreal fall/winter.

The objective of this study is 1) to examine the intrinsic evolution features of the biennial mode on a monthly basis to understand its physical mechanism, and 2) to investigate manner and extent of the impact the biennial mode exerts on the Asian-Australian monsoon precipitation. CSEOF analysis is carried out to separate the seasonal cycle and the biennial mode. This separation is best accomplished by using a long SST record as in Yeo and Kim (2014). Then, key physical variables are also analyzed in conjunction with these two modes. A main focus area (Fig. 1) is the tropical Indo-Pacific region (90°-150°E, 20°S-20°N) where the biennial variability is prominent and the seasonal migration of the Asian-Australian monsoon system is developed.

Data and methods used in this study are introduced in section2. In section 3, results based on CSEOF analysis are discussed. The evolution patterns of the biennial mode during a 2-year period and the seasonal cycle of precipitation

are described in detail, and the physical relationship among different variables is analyzed. Finally, concluding remarks are presented in section 4.

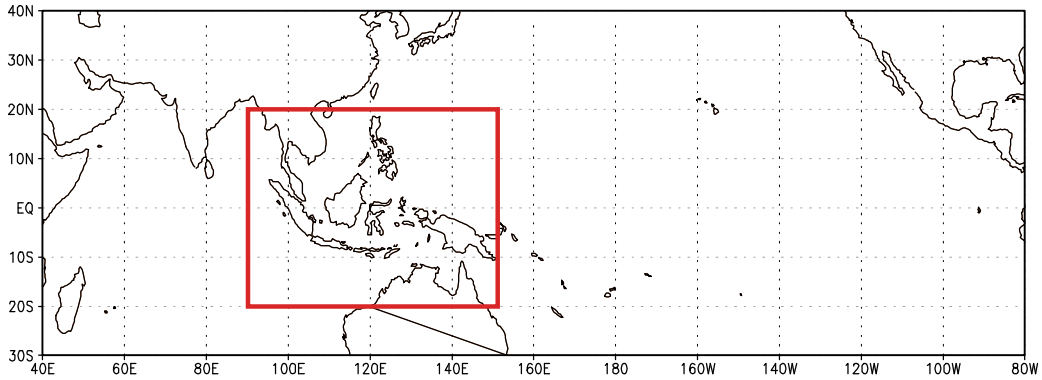

Figure 1. The main focus area of this study is the red box (90°-150°E, 20°S-20°N), and is called the tropical Indo-Pacific region in the present study.

2. Data and Method of Analysis

2.1. Data

Monthly Extended Reconstruction Sea Surface Temperature (ERSST) version 3 dataset for 103 years (1910-2012) is used in the present study; the ERSST dataset covers the near-global region (0-360°E, 46°S-60°N). In order to understand the evolutions of atmospheric variables, the Twentieth Century Reanalysis (20CR) version 2 (Compo et al. 2011) monthly datasets for the same period of time are utilized in the present study. Data at the surface and the 17 pressure levels from 1000 hPa to 200 hPa are analyzed.

2.2. CSEOF analysis

The seasonal cycle and the biennial oscillation mode are extracted from the ERSST dataset using cyclostationary EOF (CSEOF) analysis. In CSEOF analysis, spatio-temporal data are decomposed into CSEOF loading vectors (CSLVs), $B_n(r,t)$, and principle component (PC) time series, $T_n(t)$:

$$Data(r,t) = \sum_n B_n(r,t)T_n(t). \quad (1)$$

In this study, CSLV for each mode consists of 24 monthly spatial patterns evolving in time (nested period = 24 months). The first mode ($n = 1$) of the ERSST dataset represents the seasonal cycle of SST and the fourth mode ($n = 4$) denotes the biennial oscillation signal (Yeo and Kim 2014), which describes the transition from the La Niña phase to the El Niño phase in the Pacific Ocean over a two-year period.

The corresponding PC time series describes longer-term variability of the biennial mode and explains how the intensity of the biennial signal has changed in the record. CSEOF analysis is also conducted on others atmospheric variables with the same nested period (24 months).

2.3. Regression analysis in CSEOF space

The target variable in this study is sea surface temperature (SST). A multivariate regression analysis in CSEOF space is carried out to identify the variation of atmospheric variables pertaining to the SST seasonal cycle mode and the biennial oscillation mode. The regression analysis is written as

$$T_n^{sst}(t) = \sum_{m=1}^{M} \alpha_m^{(n)} T_m^{atm}(t) + \varepsilon^{(n)}(t), \tag{2}$$

where $T_n^{sst}(t)$ is the n th mode of the SST PC time series, $T_m^{atm}(t)$ is the m th PC time series of an atmospheric variable (predictor variable), $\left\{\alpha_m^{(n)}\right\}$ are the regression coefficients, $\varepsilon^{(n)}(t)$ is regression error time series, and M is the number of predictor PC time series used for regression. The regressed CSLV of an atmospheric variable, which is physically consistent with the SST evolution of the n th CSEOF mode, can be obtained via

$$B_n^{reg}(r,t) = \sum_{m=1}^{M} \alpha_m^{(n)} B_m^{atm}(r,t), \tag{3}$$

where $B_m^{atm}(r,t)$ are the original CSLVs of the predictor variable. With the regression analysis in CSEOF space, entire data collection can be rewritten as follows:

$$Data(r,t) = \sum_n \left\{ SST_n(r,t), SLP_n^{reg}(r,t), UV_n^{reg}(r,t), P_n^{reg}(r,t), \ldots \right\} T_n^{sst}(t), \qquad (4)$$

where $\left\{ SST_n(r,t), SLP_n^{reg}(r,t), UV_n^{reg}(r,t), P_n^{reg}(r,t), \ldots \right\}$ are the loading vectors of the target and predictor variables; they share the PC time series, $\left\{ T_n^{sst}(t) \right\}$, of the target variable.

The seasonal cycle and the biennial oscillation modes are the physical evolutions oscillating continuously with one-year and two-year cycles, respectively. CSEOF analysis is applied to explain their space-time evolutions, which is not described adequately with an index or a single pattern.

3. Results

3.1. The seasonal cycle of precipitation

Since the purpose of the present study is to understand how the biennial mode affects the seasonal precipitation pattern, the seasonal cycle of precipitation in the study area will be investigated first. Figure 2 shows the seasonal cycle of precipitation over the Indo-Pacific region. The spatial patterns clearly show the seasonal dependency of precipitation in both hemispheres. Precipitation begins to increase above the annual mean value in May/June in the northern hemisphere with a maximum in August. Precipitation dwindles in October over the northern hemispheric continental areas. As the precipitation band crosses the equator, monsoon precipitation increases above the annual mean value in the southern hemisphere in December. This seasonal excursion of precipitation depicts the evolution of the Asian-Australian monsoon system. This monsoon system migrates between the northeast Asia including East China, Korea and Japan and the northern Australia every year, although the meridional stretch varies from one year to another. It is noteworthy that there is a strong asymmetry in the precipitation patterns between the two hemispheres primarily because of the very distinct land-sea configurations. The corresponding PC time series shows that the amplitude of the seasonal cycle has fluctuated by about ±20% during the data period.

The seasonal cycle of precipitation, moving back and forth between the two hemispheres, is perturbed by the biennial oscillation of SSTA. One of the primary goals of this study is to understand how the biennial oscillation of SSTA interacts

with the atmospheric variables and, as a result, modulates the monsoon precipitation in time and space.

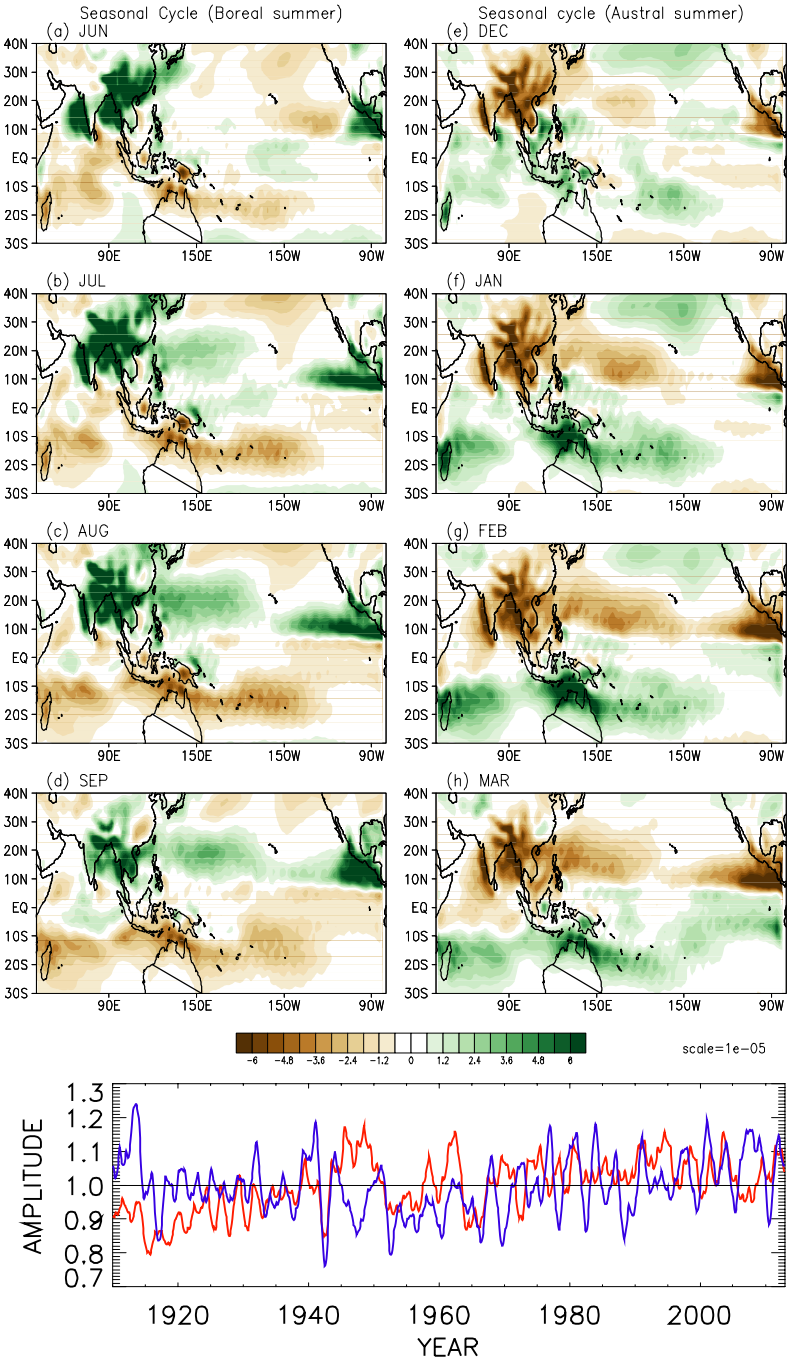

Figure 2. (top) The seasonal patterns of precipitation over the Indo-Pacific region and (bottom) the corresponding PC time series. The left column depicts the Asian Monsoon (red PC time series) and the right column the Australian Monsoon (blue PC time series).

3.2. The biennial mode of sea surface temperature

The biennial component of variability in the near global SST (0°-360°E, 46°S-60°N) was extracted via CSEOF analysis from the 103-year (1910-2012) ERSST v3 data. The biennial signal is extracted as the fourth CSEOF mode and explains about 8% of the total variance aside from the seasonal variability. As discussed in Yeo and Kim (2014), the biennial mode of SST, a prominent feature in the tropics, is one of the primary mechanisms of ENSO together with the low-frequency variability mode and the global warming mode. Figure 3 depicts the 2-year seasonal patterns of the loading vector of the biennial mode. In this study, we will call the period from May of first year to April of second year the cold phase and from May of second year to April of first year the warm phase in the biennial mode. The seasonal evolution patterns depict the evolution of warm and cold phases of SSTA and the phase transition between them. During the mature phase well-developed El Niño or La Niña patterns are seen in the tropical Pacific. The delayed action oscillator [Suarea and Schopf 1988; Battisti and Hirst 1989] and the recharge-discharge oscillator [Jin 1997a, 1997b] are suggested as the primary physical mechanism for the oscillation and transition of the biennial mode.

Negative (positive) SSTA emerges in the tropical eastern Pacific Ocean in May, while positive SSTA over tropical Indian Ocean and western Pacific has persisted from the previous fall. This negative SSTA over the eastern Pacific extends toward the central Pacific in July-September and the warm SSTA dwindles toward the east in the Indian Ocean. When the cold phase matures with strong

negative SSTA over the central-eastern Pacific, triple anomaly patterns are observed from the Indian Ocean to the Pacific Ocean with horseshoe-shaped positive SSTA over the western Pacific and basin-wide cold anomaly over the Indian Ocean. After negative SSTA reaches maximum over the tropical Pacific, SSTA over the Indian Ocean peaks during January-March. Subsequently, positive SSTA develops in the tropical eastern Pacific in the following May as the cold phase decays. The timing of the phase transition is different between the tropical Pacific Ocean (boreal spring) and the tropical Indian Ocean (boreal autumn). Eastward expansion of SSTA is also seen over the Indian Ocean and the western Pacific. These evolution patterns, particularly in summer and winter, are similar with the tropical SSTA variation in other researches except for the quasi-biennial periodicity in earlier studies (Barnett 1991; Li et al. 2006; Chung et al. 2011). The PC time series in the bottom panel of Fig. 3 shows the long-term amplitude variation of the biennial mode.

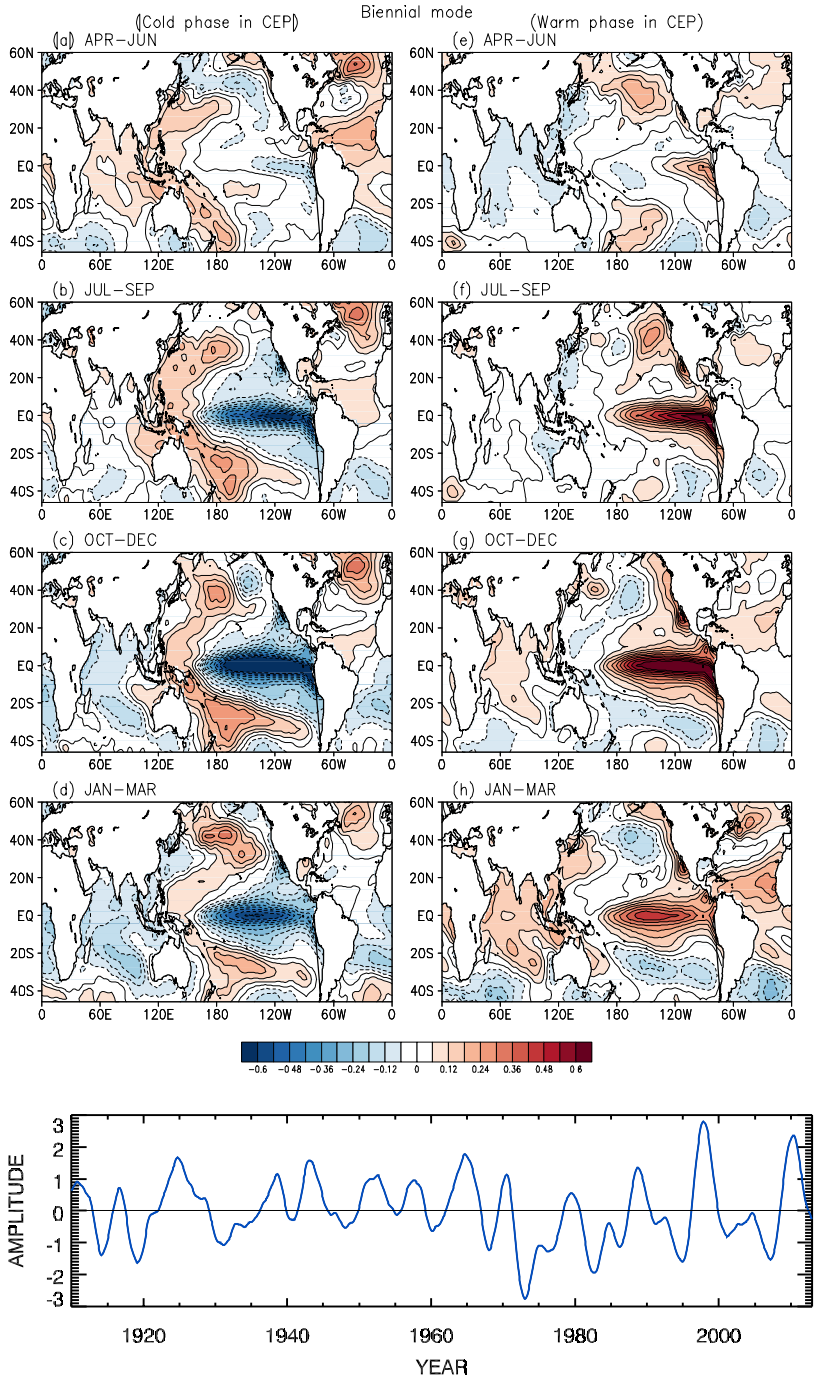

Figure 3. (top) The seasonal patterns of the CSEOF loading vector of the biennial mode derived from the near-global (0°-360°E, 46°S-60°N) sea surface temperature and (bottom) the corresponding PC time series.

3.3. Temporal evolution of the atmospheric circulation in the biennial mode

To identify atmospheric circulation and precipitation change associated with the biennial mode, atmospheric evolution patterns are obtained via regression analysis in CSEOF space. The SSTA change in the tropical central-eastern Pacific in the biennial mode directly influences the equatorial zonal circulation. Figure 4 depicts the temporal evolution of SSTA, SLPA, anomalous low-level horizontal wind and vertical velocity in the equatorial region (6°S-6°N). In the equatorial region, atmospheric change is nearly concurrent with the local SSTA evolution. A notable exception is the SLPA over the Indian Ocean and the western Pacific; it appears that SLPA in these regions is influenced by the central-eastern Pacific SSTA rather than the local SSTA. It is also observed that atmospheric anomalies propagate eastward over time, particularly in between the Indian Ocean and the central Pacific. The coherence between the change in SST and that of the atmospheric variables implies their connection through air-sea interaction. Anomalous pressure switches its sign across the central Pacific (~180°E). The sign of anomalous pressure is reversed in the western Indian Ocean about one month prior to the development of a new phase of SSTA over the tropical Pacific. The local meridional circulation (90°-150°E longitudinal average) in the biennial mode (Fig. 5) displays the seasonal variation of the vertical structure over the tropical Indo-Pacific region, which seems to be linked with the maritime continent branch of the zonal circulation (Fig. 4).

In May of the first year, the cold phase of SSTA begins to develop with the dissipation of the opposite phase in the central-eastern Pacific. During boreal spring, positive SLPA over the tropical Pacific Ocean and negative SLPA over the tropical Indian Ocean are developed in association with the east-west SSTA contrast (Fig. 4a). The upward motion persisting from the previous summer changes to a downward motion over the central-eastern Pacific. An upward motion develops over the eastern Indian Ocean and extends to the western Pacific with the intensification of the cold SSTA in the central-eastern Pacific. The downward vertical motion is connected with the low-level easterly over the equatorial Pacific and the westerly over the equatorial Indian Ocean, which is consistent with the SLPA gradient. This anomalous low-level horizontal wind is responsible for low-level wind divergence, leading to anomalous subsidence over the central Pacific Ocean, and the opposite situation over the western Pacific and the Indian Oceans. Meanwhile, anomalous anticylonic circulation remains in the western North Pacific (Fig. 5f). Anomalous low-level divergence is observed along the southern plank of the anticyclonic circulation centered around 15°N. This divergence corresponds to the descending branch of the local (90°-150°E) meridional circulation anomaly, which is linked with the upward branch of the anomalous zonal circulation in the equatorial region (see Figs. 5b and 5f). Therefore, meridional asymmetry, with a northward shift of the circulation center, is evident as the new phase of the biennial mode is developed over the equatorial region during boreal spring. Anomalies over the northern tropical region have

persisted from the previous fall without any sign change. During boreal summer, equatorial zonal circulation intensifies as cold SSTA extends and strengthens over the central-eastern Pacific. Upward motion over the western Pacific slightly migrates eastward.

For boreal fall (austral spring), anomalous westerly is developed over the Indian Ocean, which strengthens the anomalous convection centered over the Maritime Continent. This westerly results in the appearance of cold water from the western Indian Ocean (see Fig. 4a). The cold SSTA extends eastward and the warm SSTA shrinks toward the eastern Indian Ocean and the far western Pacific. The enhanced anomalous zonal wind over the Indo-Pacific region migrates eastward and the convergence center also shifts eastward to the far western Pacific. Maximum sinking motion is observed to the west of the maximum cold SSTA over the tropical Pacific, which represents the branch of the low-level divergence associated with the SLPA gradient (Figs. 4a and 4b). The center of the anomalous low over the Indian Ocean moves over the Maritime Continent (Fig. 4a) simultaneously with the basin-wide cooling in the Indian Ocean, and the enlarged low exerts stronger influence in the western Pacific. Consequently, anomalous lows (cyclonic circulations) form over the South China Sea and Australia (Fig. 5g, see also Fig. 12). The cyclonic circulation to the north moves northeastward to the western North Pacific by the following spring. This development of subtropical low is attributed to the Rossby wave type response to the anomalous convection over the western Pacific associated with the local warming (Gill 1980;

Wang et al. 2000). The subtropical low and the stronger zonal wind induce low-level convergence in the entire tropical zonal band of 90°-150°E including the northern part of Australia; this is consistent with the enhanced zonal circulation in this region (Fig. 5c).

From January to March of the second year, the negative SSTA expands toward the eastern Indian Ocean, and the whole Indian Ocean exhibits negative SSTA by March. The equatorial vertical motion begins to weaken in accordance with the decreased SSTA over the central-eastern tropical Pacific. It is also shown that the upward motion shrinks over the western Pacific, and the westerly over the Maritime Continent migrates eastward (Fig. 4b).

In the spring of the warm phase, sign of the zonal SLPA pattern is reversed, as positive SSTA develops over the eastern Pacific while cold SSTA persists over the Indian Ocean. During the warm phase, the anomalous evolution patterns are reversed in sign.

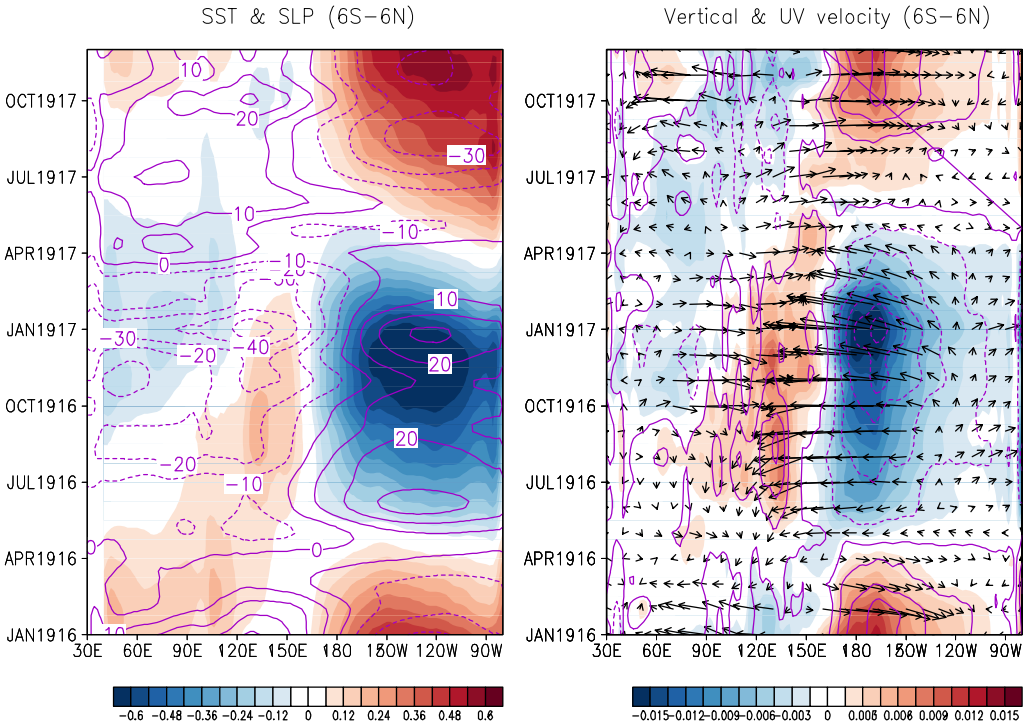

Figure 4. (left) Longitude-time plot for SSTA (shading) and SLPA (contour) in the equatorial region (6°S–6°N). (Right) Longitude-time plot for vertically averaged (850–200 hPa) vertical velocity (shading), low-level (1000–850 hPa) equatorial horizontal wind (vector), and (contour) horizontal wind convergence in the equatorial region (6°S–6°N).

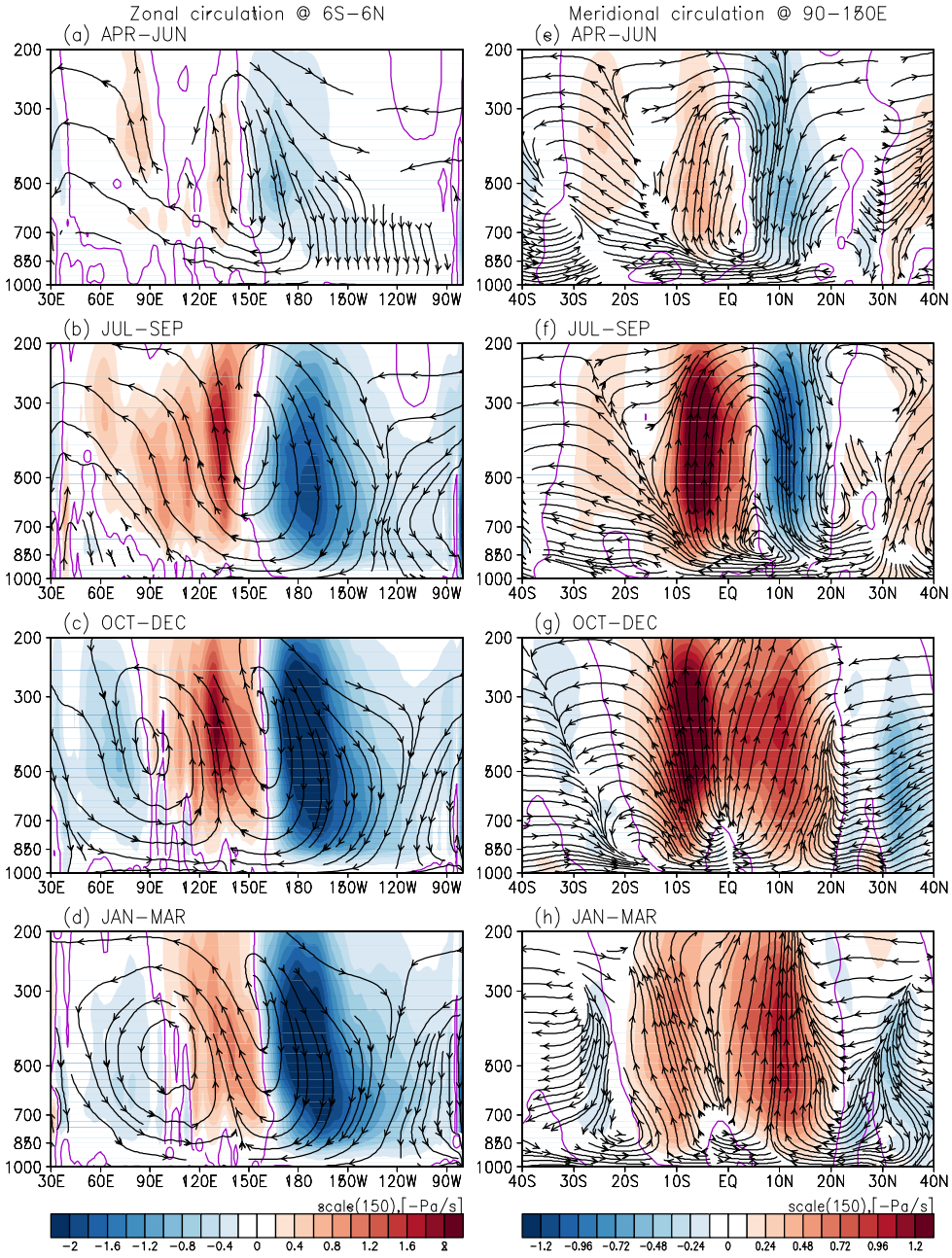

Figure 5. Seasonal evolution patterns of the zonal circulation in the latitude band of 6°S-6°N (left panels), and the meridional circulation in the zonal band of 90°-150°E (right panels) for the cold phase of the biennial mode. Shading denotes the vertical velocity (–pa s^{-1}). During the positive phase of the biennial mode, the situation reverses.

3.4. Change in moisture flux and precipitation in the biennial mode

The anomalous low-level circulation induced by the biennial mode alters moisture transport. Considering that the seasonal cycle and the biennial mode of SSTA both influence the temporal evolution of moisture and wind, anomalous moisture flux is calculated from

$$q\vec{u} - \overline{q\vec{u}} = (\overline{q} + q')\left(\overline{\vec{u}} + \vec{u}'\right) - \overline{(\overline{q} + q')\left(\overline{\vec{u}} + \vec{u}'\right)}$$

$$= \overline{q}\vec{u}' + q'\overline{\vec{u}} + q'\vec{u}' - \overline{q'\vec{u}'}, \qquad (5)$$

where $\overline{q}$ and $\overline{\vec{u}}$ represent the climatology of moisture and wind, while q' and $\vec{u}'$ denote anomalous moisture and wind induced by the biennial mode. Then, the convergence of anomalous moisture flux is given by $-\nabla \cdot \left(\overline{q}\vec{u}' + q'\overline{\vec{u}} + q'\vec{u}' - \overline{q'\vec{u}'}\right)$. Figure 6 shows the patterns of moisture convergence and vertical motion during the cold phase of the biennial mode. This figure shows that the pattern of the vertical velocity induced by the convergence of low-level wind (assuming that the atmosphere is nearly incompressible on a monthly scale) is nearly identical with the pattern of moisture convergence calculated according to (5). This indicates that the first term in (5) explains the majority of moisture convergence in the lower troposphere, and implies that the variation of the low-level wind is more crucial than that of specific humidity in explaining the moisture transport change associated with the biennial oscillation of SSTA.

Figure 7 shows that the anomalous precipitation induced by the biennial

mode, particularly in the tropics, is highly correlated with the anomalous vertical motion and anomalous moisture convergence. This means that the change in moisture convergence accompanied by vertical motion is the primary mechanism of the variation in precipitation rate. Figures 8 and 9 describe the anomalous precipitation rate associated with the SSTA biennial oscillation in summer (JJAS) of each hemisphere. It is observed that precipitation over the tropical region is more sensitive to the biennial variation of SSTA, since SSTA variation is primarily confined to the tropics. The influence of the biennial mode is weaker in higher latitudes. This biennial variability in the precipitation rate within the zonal band of 90°-150°E explains about 9% and 11% of the total variance aside from the seasonal cycle in the northern and southern tropical regions, respectively. In general, low-level moisture convergence (divergence) combined with upward (downward) motion provides a favorable (unfavorable) condition for precipitation. In boreal summer with negative SSTA in the central-eastern Pacific, the ascending branch of anomalous meridional circulation in the zonal band of 90°-150°E is confined to the equatorial region (Fig. 5f), and the low-level moisture divergence in the northern tropics induces a dry condition (Figs. 8a-c).

In austral summer, negative precipitation anomaly over the northern tropics disappears and positive precipitation anomaly in the equatorial region extends to the whole tropics in the 110°-160°E zonal band including the northern part of Australia (Figs. 8e-g). This wet condition is related to an upward branch of the enhanced and enlarged zonal circulation with low-level moisture convergence

due to the intensified negative SSTA forcing over the tropical Pacific. Compared with the boreal summer, the center of the anomalous precipitation over the Indo-Pacific region is located closer to the equator as can also be seen in the local meridional circulation (see Figs. 5f and 5h).

As discussed above, the biennial mode affects the Asian-Australian monsoon system, which features the seasonal migration of precipitation band between the two hemispheres over the Indo-Pacific. To understand the impact of the biennial mode on the Asian-Australian monsoon system in a precise manner, the biennial mode should be considered together with the seasonal cycle (Fig. 2). The meridional range of migration of precipitation band is narrower in the biennial mode than in the seasonal cycle. Besides the tropical region, weak biennial variability appears over the subtropical China but its location varies in time. In the boreal summer of the cold phase, when the seasonal cycle of precipitation band resides in the northern hemisphere (Figs. 2a-d), precipitation decreases over the northern tropics (the Bay of Bengal, the Indochina peninsula, the South China Sea and the Philippine Sea) and increases in the mid-latitude eastern and central China (Figs. 8a-d). In the austral summer of the cold phase, when the seasonal precipitation band lies in the southern hemisphere (Figs. 2e-h), the positive precipitation anomaly over the northern part of Australia makes monsoon precipitation stronger and also the onset of Australian rainy season earlier (Figs. 8e-h). In the boreal summer of the warm phase, precipitation in the northern tropics is intensified and precipitation in the subtropical China is weakened.

Precipitation induced by the biennial mode is weaker and is tightly confined to the tropics in August and September (Figs. 9a-d). In the austral summer of the warm phase, negative anomaly over the northern part of Australia leads to a delayed onset of the rainy season and also less precipitation throughout the rest of the Australian rainy season (Figs. 9e-h). As is evident in Figs. 8 and 9, the impact of the biennial mode is dramatically different between the two hemispheres, since the SSTA and the ensuing atmospheric circulation differ significantly during the rainy seasons in the two hemispheres. It should also be noted that precipitation induced by the biennial mode is reasonably symmetric between the cold and warm phases.

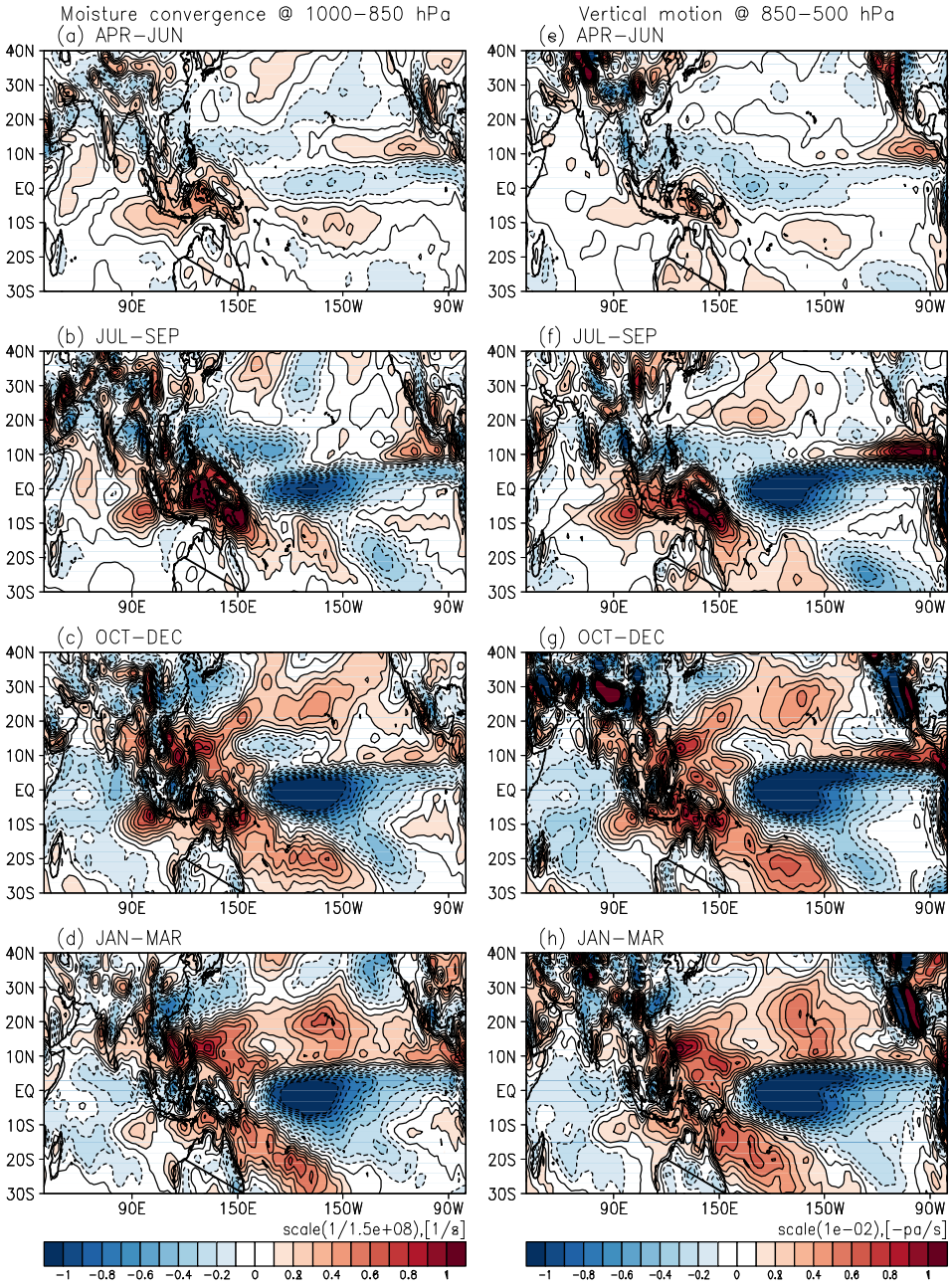

Figure 6. Spatial patterns of moisture convergence (left column) and vertical motion (right column) during the cold phase (La Niña year) of the biennial mode.

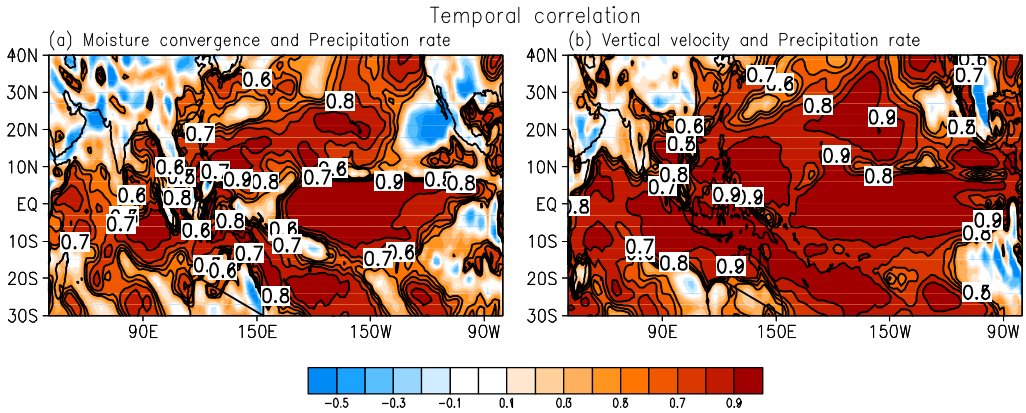

Figure 7. Map of correlation between the precipitation rate and moisture convergence (left), and omega velocity (right) in the biennial mode.

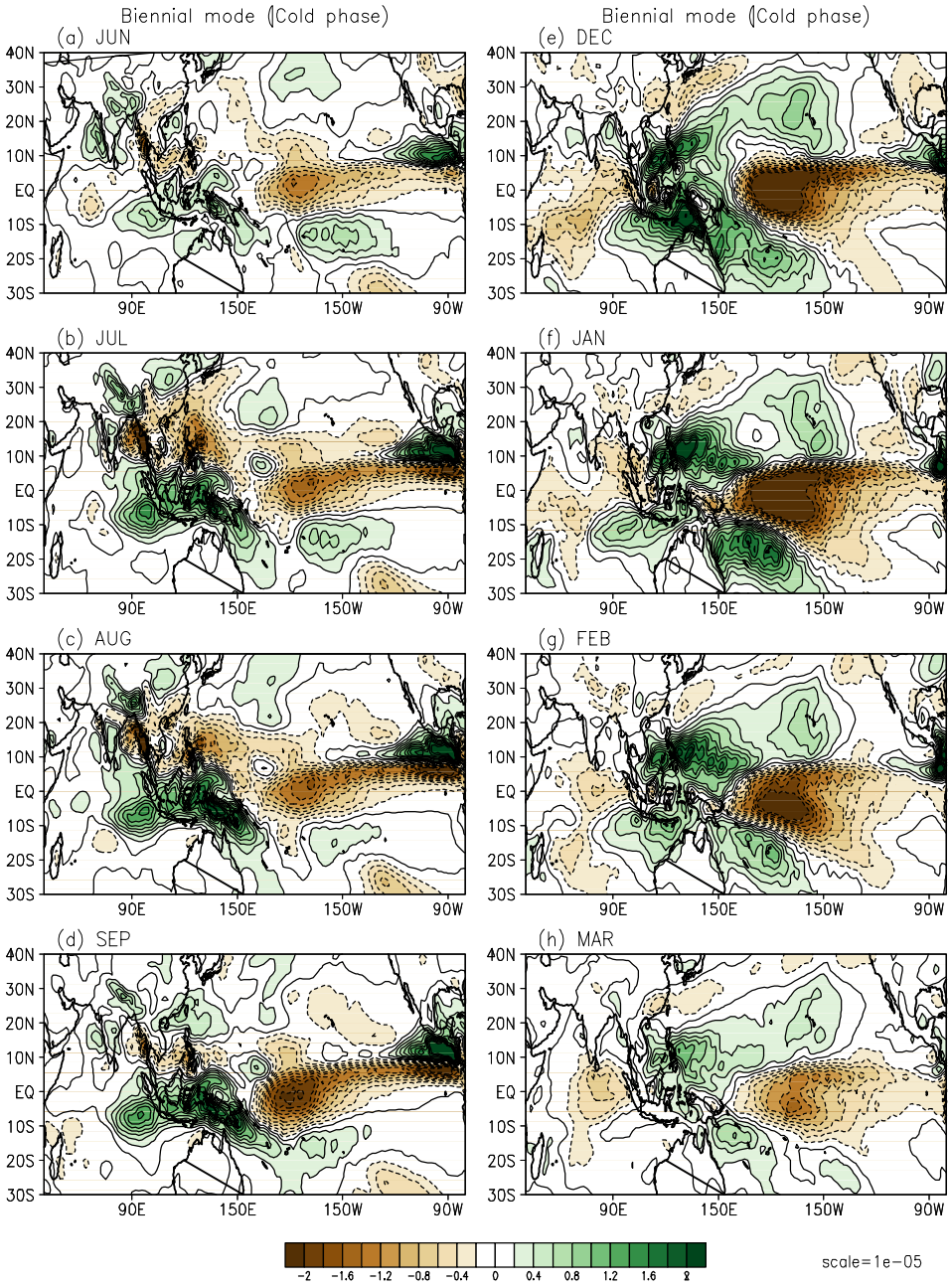

Figure 8. Anomalous precipitation rate for the cold phase of the biennial mode during boreal summer (June-September) and austral summer (December-March).

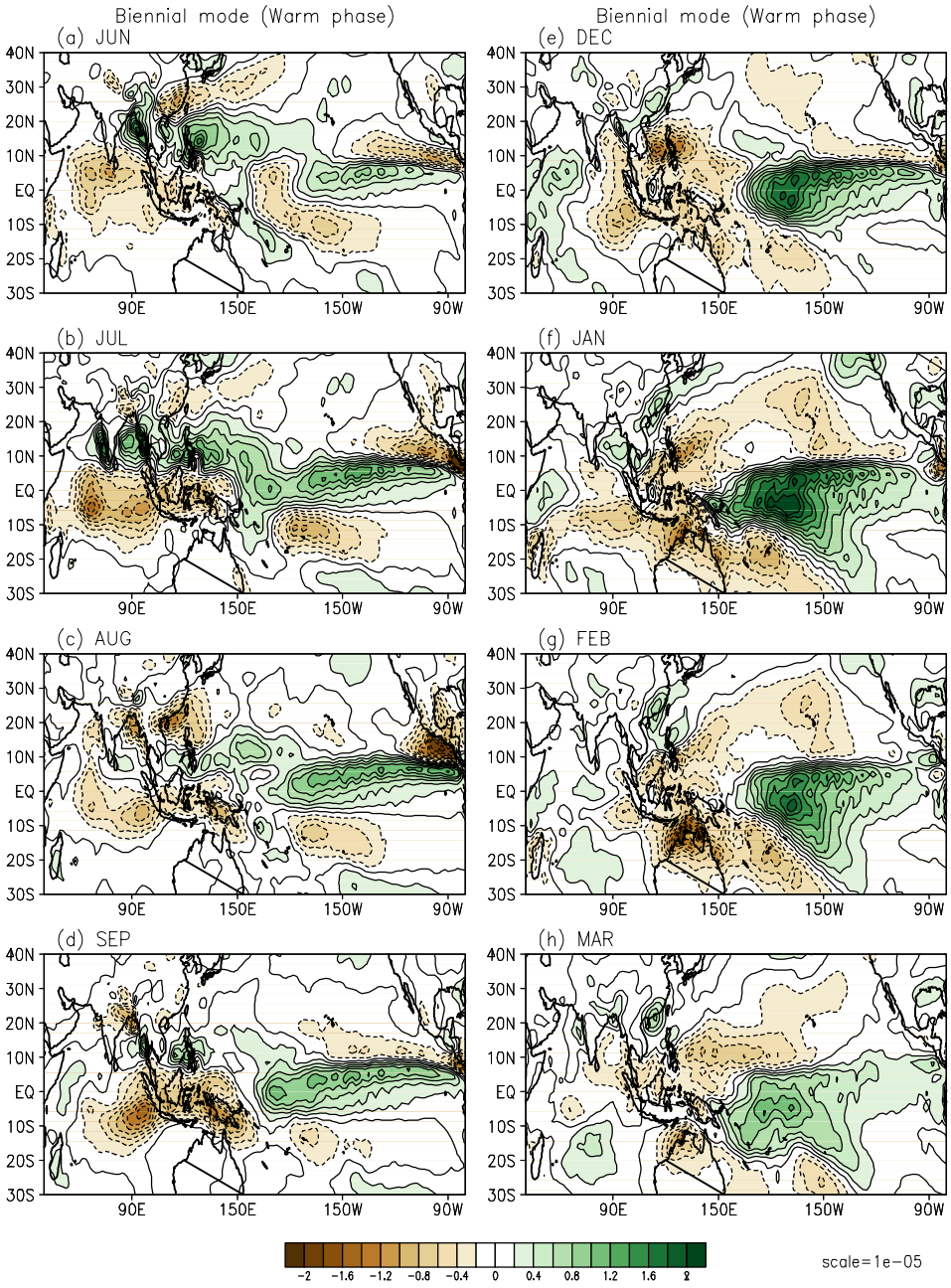

Figure 9. Anomalous precipitation rate for the warm phase of the biennial mode during boreal summer (June-September) and austral summer (December-March).

3.5. Difference in the biennial response between the two hemispheres

It is realized that the precipitation response over the Indo-Pacific region to the biennial oscillation of SSTA differs significantly between the boreal summer and the austral summer. In boreal summer, the sign of precipitation anomalies over the tropical Indian Ocean and the Maritime Continent is opposite to that over the Bay of Bengal, the Indochina peninsula, the South China Sea, and the Philippine Sea. In austral summer, however, the sign of precipitation anomaly is the same over the whole tropical region from the eastern Indian Ocean to the western Pacific Ocean (the tropical Indo-Pacific region). A plausible explanation for this difference is in the relative size and intensity of the central and eastern Pacific SSTA and the different timing of SSTA phase transition over the Pacific Ocean and the Indian Ocean.

In boreal summer, SSTA over the central and eastern Pacific is not wide and strong enough to exert influence on the whole tropics over the tropical Indo-Pacific region; atmospheric variables respond directly to SSTA near the equator only. Change in the northern tropical region is attributed to the anomalous local meridional circulation, which is linked to the equatorial zonal circulation. On the other hand, a remote forcing of maximum SSTA influences broader tropics via zonal circulation in austral summer.

Figure 10 shows that the new phase of the basin-wide SSTA over the Indian Ocean appears in September and the new phase over the Pacific Ocean appears in

May. Due to the different timing of the phase transition between the two oceans, SST anomalies of opposite signs are observed over the tropical oceans (Fig. 3) for boreal summer (green stripe in Fig. 10): one sign over the central-eastern Pacific and the other sign over the western Pacific and the Indian Ocean. During austral summer, SSTA over the Indian Ocean and that over the central-eastern Pacific are of identical sign separated by the SSTA of opposite sign in the western Pacific. The anomalous pressure pattern is relocated accordingly, accompanied by a noticeable change in the low-level circulation over the northern tropics. Figure 11 indicates that the phase transition of anomalous low-level pressure and anomalous wind over the northern tropics occurs in September/October, which is nearly concurrent with the transition of the Indian Ocean SSTA. This implies that the anomalies over the northern tropical region (in the vicinity of the Indochina Peninsula and the western North Pacific Ocean) are related to the SSTA change over the Indian Ocean.

Figure 12 represents the atmospheric patterns of the biennial mode in boreal summer (June-September) and austral summer (November-February). Anomalous low is observed in the Indian Ocean and anomalous high in the Pacific Ocean when warm SSTA exists from the Indian Ocean to the western Pacific and cold SSTA is present in the central-eastern Pacific Ocean in boreal summer (Fig. 11a). In accordance with the anomalous pressure change, anomalous easterly develops over the Bay of Bengal, the South China Sea and the Philippine Sea and also anomalous anticylonic circulation lies over the western North Pacific. This anticylonic circulation developed in the previous austral summer in response to

local SSTA forcing. It appears that the residual warm SSTA in the Indian Ocean is an important factor for its maintenance (Fig. 11). Some studies (Wu et al. 2009; Wu et al. 2010; Yuan et al. 2012; Yang et al. 2007; Xie et al. 2009) regard it as the Kelvin wave type response to the basin-wide warming in the Indian Ocean. The anomalous easterly along the southern plank of the anticyclonic circulation generates low-level wind divergence in the northern tropical region, which is physically interlocked with the downward branch of the local meridional circulation (Fig. 5f) forced by the convection on the maritime continent (Chung et al. 2011; Wu et al. 2009).

As the new phase of the Indian Ocean SSTA is developed in austral summer, cold SSTA in the Indian Ocean contributes to the extension of the anomalous low as its center migrates toward the western Pacific. Then, the anomalous anticyclonic circulation over the western North Pacific disappears and cyclonic circulation is established on both sides of the equator in the tropical Indo-Pacific region, which looks similar to the Rossby wave type response (Taschetto et al. 2010; Yuan et al. 2012; Wang et al. 2000; Wu and Kirtman 2004b) to the local warming and the remote forcing by strong central-eastern Pacific cooling. Also the anomalous easterly in the northern tropics changes to westerly so that anomalous westerly dominates from the Indian Ocean to the central Pacific in both the northern and southern tropics. Thus, a combination of the tropical zonal wind and the cyclonic circulations in both hemispheres encourages the development of low-level wind convergence over the tropical Indo-Pacific. Meanwhile, the intensified and

widened cold SSTA in the central-eastern Pacific strengthens the local descending motion and it remotely strengthens the ascending motion over the tropical Indo-Pacific region. The downward motion over the equatorial Indian Ocean also helps strengthening the ascending motion over the tropical Indo-Pacific. The upward motion exists over the whole tropical region within the zonal band of 90°-150°E in connection with the low-level wind convergence induced by the cold SSTA in the central-eastern Pacific and the Indian Ocean.

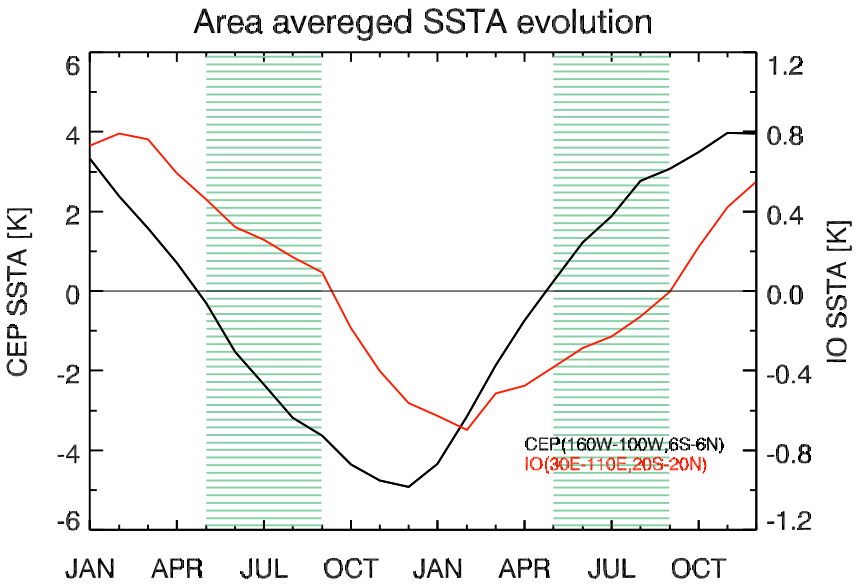

Figure 10. Time evolution of area-averaged SSTA over (black) the central eastern Pacific (160°-100°W, 6°S-6°N) and (red) Indian Ocean (30°-110°E, 20°S-20°N). Green shading indicate the time gap of their phase transition.

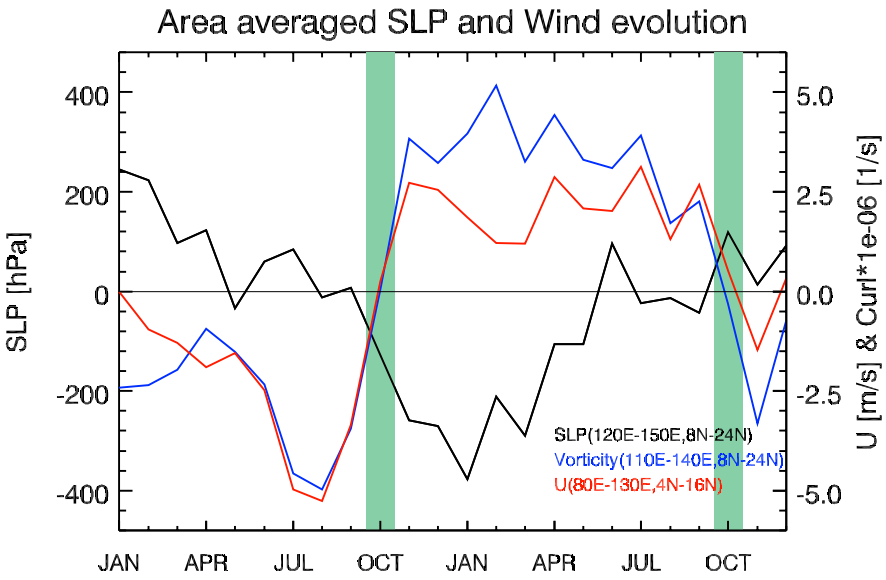

Figure 11. Time evolution of the local (120°-150°E, 8°-24°N) SLPA (black) and the local (110°-140°E, 8°-24°N) vorticity (blue) over the western North Pacific and anomalous zonal wind (red) over the northern Indian Ocean (80°-130°E, 4°-16°N) in the biennial mode. The green bars denote the times when the anomalies change the sign.

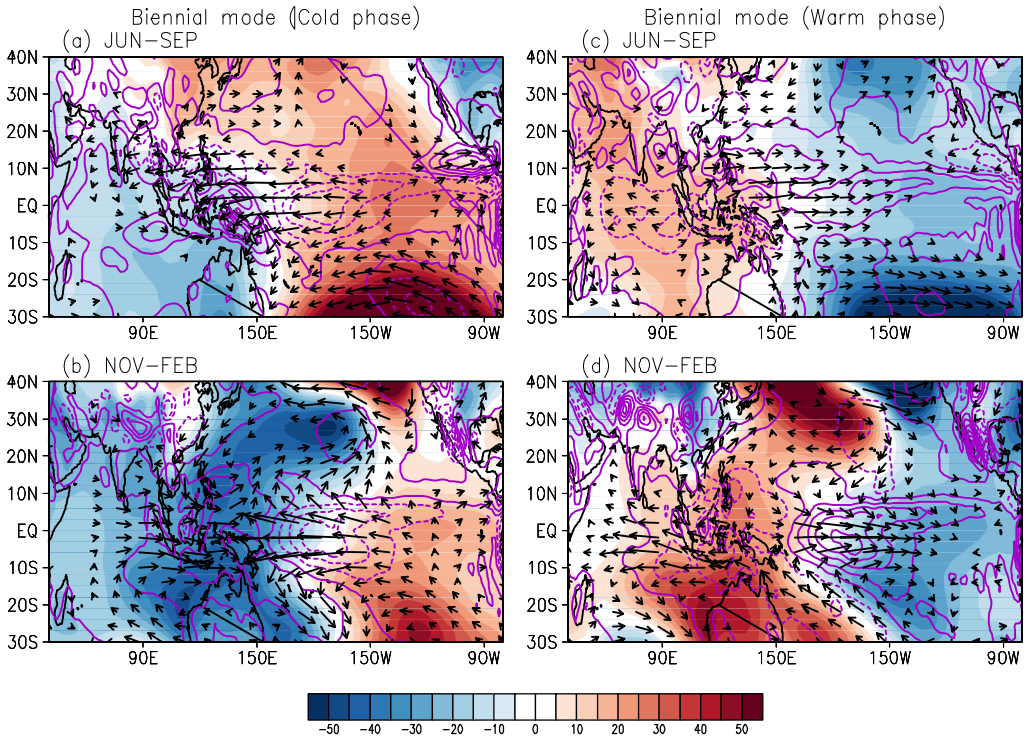

Figure 12. The 4-month averaged low-level (1000–850 hPa) horizontal wind (vector), SLPA (shading), and column-averaged (850–200 hPa) vertical velocity (contour) of the biennial mode for boreal summer (upper panels) and austral summer (lower panels).

4. Concluding remarks

It was scrutinized how atmospheric variables change in accordance with each other in the biennial oscillation of SSTA via CSEOF analysis. The impact of the biennial SST variation on the Asian-Australian monsoon system was investigated based on the seasonal cycle of precipitation and the spatial patterns of various variables associated with the biennial mode. It should be noted that the contribution of the biennial mode was examined independently of the seasonal cycle so that the temporal evolution induced by the biennial mode could be clearly distinguished from the temporal evolution arising from the seasonal cycle. The result shows that the two-year cycle variability induced by the biennial oscillation of SSTA is relatively insignificant in higher latitudes but is significant over the tropical region particularly in the 90°-150°E zonal band. Precipitation in the tropics changes significantly according to the low-level moisture convergence and vertical motion induced by the SSTA biennial oscillations. It is confirmed that the anomalous horizontal wind is much more instrumental in the low-level moisture flux change than the anomalous specific humidity under the SSTA biennial rhythm.

Biennial variability reflected in the atmospheric variables and precipitation over the tropical Indo-Pacific region (90°-150°E, 20°S-20°N) features significantly different response patterns between boreal summer and austral summer. The source of this difference is in the tropical Indo-Pacific region, which, on the other hand, is influenced in a complicated way by both the Pacific and the Indian Oceans. Generally, the northern tropical atmospheric anomalies tend to

follow the evolution of the Indian Ocean SSTA, whereas the equatorial and southern tropical anomalies tend to follow that of the central-eastern Pacific SSTA (maximum correlation at lag 0). The intensity and size of SSTA over the central-eastern Pacific Ocean and the timing of SSTA transition in the Pacific Ocean and the Indian Ocean are considered as key factors for this; they result in distinct seasonal dependency in the two-year cycle variations of the atmospheric variables and precipitation over the tropical Indo-Pacific region. The atmospheric responses over the tropics are dynamically connected via the anomalous zonal circulation and the local meridional circulation. In boreal summer, anomalous local meridional circulation is conspicuous over the tropical Indo-Pacific region, whereas the anomalous tropical zonal circulation is more dominant in austral summer.

Figure 13 depicts simplified schematics of the circulation and the SSTA changes in the cold phase of the biennial mode. During JJAS, relatively narrow and weak SSTA over the central-eastern Pacific and the residual SSTA over the tropical Indian Ocean induce air-sea interaction via equatorial zonal circulation and local meridional circulation. The northern branch (6°-20°N) of the local meridional circulation is linked to the low-level anticyclonic circulation due to the anomalous high over the western North Pacific. During NDJF, relatively wide and strong SSTA over the central-eastern Pacific and the new phase of the basin-wide SSTA over the tropical Indian Ocean result in air-sea interaction via intensified zonal circulation. To the north and south of the upward branch of the zonal circulation, low-level cyclonic circulations develop as the Rossby wave type response to the western

Pacific warming. The ensuing SLPA pattern also helps the development of the low-level cyclonic circulations. Accordingly, the downward motion and low-level moisture divergence in the northern tropics accompanies the negative precipitation anomaly during boreal summer, and the upward motion and low-level moisture convergence in the southern tropics produces positive precipitation anomaly during austral summer. It should be noted that there exists strong asymmetries in the two hemispheres, not only because of the seasonal dependency of SSTA in the tropics but also because of the different types of atmospheric responses arising from the SSTA forcing. In the warm phase, the situation reverses.

The perturbation induced by the biennial mode affects the seasonal cycle of the Asian-Australian monsoon system. During the cold phase, precipitation is reduced in the northern tropics, and precipitation is increased with an earlier onset of monsoon in Australia. During the warm phase, on the other hand, the monsoon precipitation features intensified precipitation in the northern tropics and a delayed onset and weakened precipitation in northern Australia.

In earlier studies, spectral analysis has often been used to identify the quasi-biennial tendency in the precipitation data. Many studies conclude that there is no strict 2-year periodicity in the precipitation data. Figure 14a shows the AR spectrum of the 15-36 month band-pass filtered domain-averaged precipitation. Both the time series averaged over the northern (90°-150°E, 5°-20°N) and southern (100°-150°E, 20°-5°S) tropical regions exhibit conspicuous spectral peaks at 2.3, 1.7, and 1.4 years. Figure 14b shows the AR spectra of the

biennial mode PC time series identified from the SSTA, and the domain-averaged precipitation time series in the northern and southern regions. As can be seen in the figure, the spectral content of the PC time series of the domain-averaged precipitation time series is similar to that of the SSTA biennial mode even without any regression analysis in CSEOF space. The AR spectra of the PC time series exhibit two major spectral peaks at 11.4 and 4.8 years. These are the spectral peaks of the amplitude time series modulating the biennial oscillation with a 2-year period. As a result of modulation, then, we expect peaks at

$$\omega_1 = \omega_b + \omega_a \qquad \text{and} \qquad \omega_2 = \omega_b - \omega_a, \tag{6}$$

where ω_1 and ω_2 are the two new frequencies generated due to the frequency of the PC time series ω_a modulating the biennial frequency ω_b ($\omega_b = 0.5$ yr^{-1}). It can be easily verified that the periods corresponding to (ω_1, ω_2) are approximately 1.7 and 2.4 years for the modulation period of 11.4 years and are approximately 1.4 and 3.4 years for the modulation period of 4.8 years. Figure 14a shows the three of these peaks clearly with the peak corresponding to the longest period (3.4 years) is missing; the longest peak is missing, since the time series was high-passed filtered with a cutoff frequency of 3 years. Judging from the fact that SSTA associated with the biennial mode is strongly phase-locked to the calendar months, it is reasonable to assume that the periodicity of the biennial mode is 2 years.

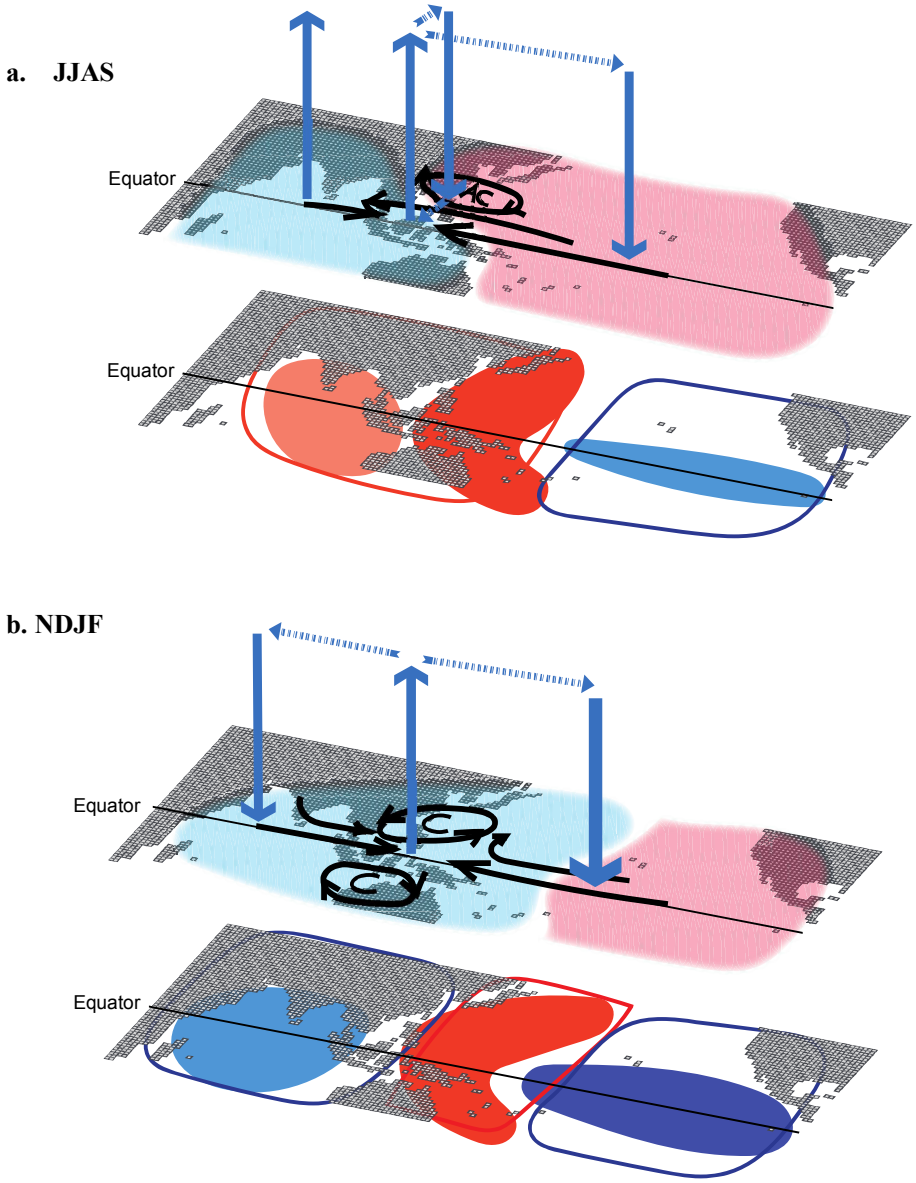

Figure 13. Schematic diagram of circulation (upper) and SSTA (lower) change in the cold phase of the biennial mode in (**a**) JJAS and (**b**) in NDJF. (upper panel) Pink shading indicates anomalous high and light blue shading indicates anomalous low. Blue vectors denote vertical circulation and upper-level wind. Black arrows represent anomalous low-level horizontal circulation. (lower panel) Red shading means warm SSTA and blue shading cold SSTA. Orange (cyan) implies that SSTA is weaker than that for red (blue).

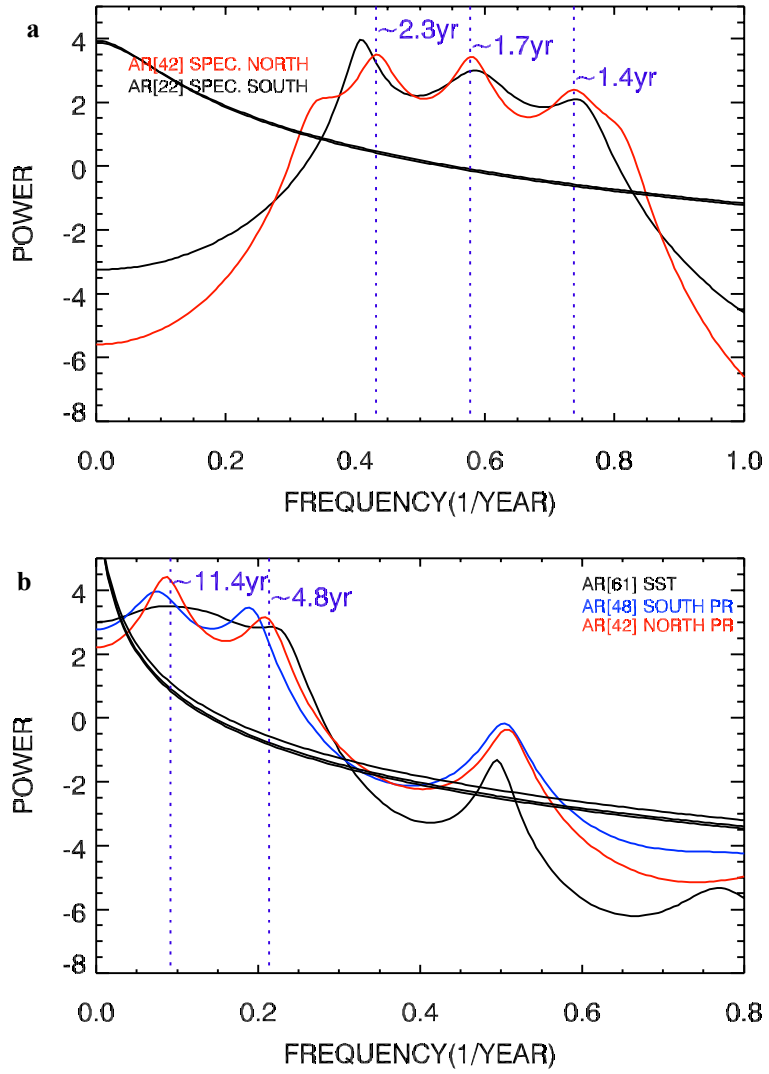

Figure 14. Auto-regressive spectral density of (a) the area-averaged precipitation anomaly over the northern (90°-150°E, 5° -20°N) and southern tropical region (100°-150°E, 20°-5°S) after the 15-36 month band-pass filter, and (b) the PC time series of precipitation for the biennial mode of SSTA and those of the precipitation averaged over the northern and southern regions.

Reference

An, Z. et al., 2014: Global Monsoon Dynamics and Climate Change. *Annu. Rev. Earth Planet. Sci.,* **43,** 2.1-2.49, doi: 10.1146/annurev-earth-060313-054623

Barnett, T. P., 1991: The interaction of multiple time scales in the tropical climate system. *J. Climate,* **4,** 269-285.

Battisti D. S., and A. C. Hirst, 1989: Interannual variability in a tropical atmosphere-ocean model: Influence of the basic state, ocean geometry, and nonlinearity. *J. Atmos. Sci.,* **46,** 1687-1712.

Chang, C.-P., and T. Li, 2000: A theory for the tropical tropospheric biennial oscillation. *J. Atmos. Sci.,* **57,** 2209-2224.

Chung, P.-H., C.-H. Sui, and T. Li, 2011: Interannual relationship between the tropical sea surface temperature and summertime subtropical anticyclone over the western North Pacific. *J. Geophys. Res.,* **116,** D13, doi:10.1029/2010JD015554

Clarke, A. J., X. Liu, and S. Van Gorder, 1998: Dynamics of the Biennial Oscillation in the Equatorial Indian and Far Western Pacific Oceans. *J. Climate,* **11,** 987-1001.

Compo et al., 2011: The Twentieth Century Reanalysis Project. *Quart. J. Roy. Meteor. Soc.,* **137,** 1-28

Gill, A.E, 1980: Some simple solutions for heat-induced tropical circulation. *Quart. J. Roy. Soc.,* **106,** 447-462.

Li, T., P. Liu, X. Fu, B. Wang, and G. A. Meehl, 2006: Spatiotemporal Structures and

Mechanisms of the Tropospheric Biennial Oscillation in the Indo-Pacific Warm Ocean Regions, *J. Climate,* **19,** 3070-3087.

Liu, Y., Y. H. Ding, H. Gao, and W. Li, 2013: Tropospheric biennial oscillation of the western Pacific subtropical high and its relatioships with the tropical SST and atmospheric circulation anomalies. *Chin. Sci. Bull.,* **58,** 364-3672.

Liu, Y., Z. –Z. Hu, A. Kumar, P. Peng, D. C. Collins, and B. Jha, 2014: Tropospheric biennial oscillation of summer monsoon rainfall over East Asia and its association with ENSO. *Climate Dyn.,* doi: 10.1007/s00382-014-2429-5

Jin F.F, 1997a: An equatorial ocean recharge paradigm for ENSO. Part I: Conceptual model. *J. Atmos. Sci.,* **54,** 811-829.

Jin F.F, 1997b: An equatorial ocean recharge paradigm for ENSO. Part II: A stripped-down coupled model. *J. Atmos. Sci.,* **54,** 830-847.

Kim, K. -Y., 2002: Investigation of ENSO variability using cyclostationary EOFs of observational data. *Meteor. Atmos. Physics,* **81,** 149-168

Meehl, G. A., 1987: The annual cycle and interannual variability in the tropical Pacific and Indian Ocean region. *Mon. Wea. Rev.,* **115,** 27-50.

Meehl, G. A., 1994: Coupled land-ocean-atmosphere processes and South Asian monsoon variability. *Science,* **266,** 263-267.

Meehl, G. A., 1997: The South Asian monsoon and tropospheric biennial oscillation. *J. Climate,* **10,** 1921-1943.

Meehl, G. A., and J. M. Arblaster 2002: The tropospheric biennial oscillation and Asian-Australian monsoon rainfall. *J. Climate,* **15,** 722-744.

Meehl, G. A., J. M. Arblaster, and J. Loschnigg, 2003: Coupled ocean-atmosphere dynamical processes in the tropical Indian and Pacific Ocean regions and the TBO. *J. Climate,* **16,** 2138-2158.

Meehl, G. A., and J. M. Arblaster, 2002: The tropospheric biennial oscillation and Asian-Australian monsoon rainfall. *J. Climate,* **15,** 722-744.

Pillai. P. A., and K. Mohankumar, 2008: Local Hadley circulation over the Asian monsoon region associated with the tropospheric Biennial Oscillation. *Theor. Appl. Climatol.,* **91,** 171-179.

Rasmusson, E. M., X. Wang, and C. F. Ropelewski, 1990: The biennial component of ENSO variability. *J. Climate,* **5,** 594-614.

Shen, S., and K. –M. Lau, 1995: Biennial oscillation associated with the East Asian summer monsoon and tropical sea surface temperatures. *J. Meteor. Soc. Japan,* **73,** 105-124.

Suarez M. J., and P. S. Schopf, 1988: A delayed action oscillator for ENSO. *J. Atmos. Sci.,* **45,** 3283-3287.

Taschetto, A. S., R. J. Haarsma, A. S. Gupta, C. C. Ummenhofer, K. J. Hill, and M. H. England, 2010: Australian Monsoon Variability Driven by a Gill–Matsuno-Type Response to Central West Pacific Warming. *J. Climate*, **23**, 4717–4736.

Trenberth, K. E., D. P. Stepaniak, and J. M. Caron, 2000: The global monsoon as seen through the divergent atmospheric circulation, *J. Climate,* **13,** 3969-3993.

Wang, B., R. Wu, and X. Fu, 2000: Pacific-East Asian teleconnection: How does ENSO affect East Asian climate? *J. Climate,* **13,** 1517-1536.

Wang, B., R. Wu, and K.-M. Lau, 2001: Interannual Variability of the Asian Summer Monsoon: Contrasts between the Indian and the Western North Pacific-East Asian Monsoons, *J. Climate,* **14,** 4073-4090.

Wang, P., B. Wang, H. Cheng, J. Fasullo, Z. T. Guo, T. Kiefer, and Z. Y. Liu, 2014: The global monsoon across timescales: coherent variability of regional monsoons, *Clim. Past*, **10,** 2007-2052.

Wang, P., 2009: Global monsoon in a geological perspective, *Chin. Sci. Bull.,* **54,** 1-24.

Webster, P.J., and V. O. Magaña, T. N. Palmer, R. A. Thomas, M. Yanai, and T. Yasunari, 1998: Monsoons: Processes, predictability, and the prospects for prediction. *J. Geophys. Res.,* **103**, 14451-14510.

Wu, R., and B. P. Kirtman, 2004a: Impacts of the Indian Ocean on the Indian summer monsoon-ENSO relationship. *J. Climate,* **17,** 3037-3054.

Wu, R., and B. P. Kirtman, 2004b: The Tropospheric Biennial Oscillation of the Monsoon-ENSO System in an Interactive Ensemble Coupled GCM. *J. Climate*, **17**, 1623–1640.

Wu, B., T. Zhou, and T. Li, 2009: Seasonally Evolving Dominant Interannual Variability Modes of East Asian Climate. *J. Climate*, **22**, 2992–3005.

Wu, B., T. Li, and T. Zhou, 2010: Relative Contribution of the Indian Ocean and Local SST Anomalies to the Maintenance of the Western North Pacific Anomalous Anticyclone during the El Nino Decaying Summer. *J. Climate,* **23,** 2974-2986.

Xie, S. P., H. Jan, T. Hiroki, D. Yan, T. Sampe, K. Hu, and G. Huang, 2009: Indian Ocean capacitor effect on Indo–Western Pacific climate during the summer

following El Niño. *J. Climate,* **22,** 2992-3005.

Yang, J. L., Q. Y. Li, S. P. Xie, Z. Y. Liu, and L. X. Wu , 2007: Impact of the Indian Ocean SST basin mode on the Asian summer monsoon. *Geophys. Res. Letter,* **34,** L02708, doi:10.1029/2006GL028571.

Yeo, S. -R. and K. -Y. Kim, 2014: Global warming, low-frequency variability and biennial oscillation: an attempt to understand the physical mechanisms, *Climate Dyn.,* **43,** 771-786.

Yuan, Y., S. Yang, and Z. Zhang, 2012: Different Evolutions of the Philippine Sea Anticyclone between the Eastern and Central Pacific El Niño: Possible Effects of Indian Ocean SST. *J. Climate*, **25**, 7867–7883.

국 문 초 록

해수면 온도의 격년 진동과 관계된
열대 인도-태평양 지역에서의 대기 순환장 및 강수장

본 연구에서는 해수면 온도 편차의 격년 진동과 관련된 인도-태평양 지역에서의 대기 순환 및 강수의 시공간적 패턴을 분석하였다. 또한 강수 밴드의 두 반구 간 계절적 이동으로 특징되는 아시아-호주 몬순 강수가, 격년변동 모드에 의하여 어떻게 조정되는지도 살펴보았다. 아시아-호주 몬순 강수에 미치는 격년변동 모드의 영향을 알아보고자, 주기정상적 경험 직교함수 (CSEOF) 분석 기법을 사용하여 해수면 온도 편차와 주요 대기 변수들에서 2 년 주기 변동성과 계절 변동성을 분리하였다. 본 연구에서 사용한 자료는 모두 월별 자료이며, ERSST 버전 3 의 해수면 온도 자료와 20 세기 재분석 자료의 대기 변수 및 강수 자료를 사용하였다. 대기 변수들의 2 년 주기 변화가 두드러지고 아시아-호주 몬순 강수의 이동 경로에 해당하는 중앙 인도-태평양 지역 (90°-150°E, 20°S-20°N) 을 중점적으로 살펴보았다. 북반구 여름철의 경우, 중앙 인도-태평양 지역에서 지역 남북 순환장이 특징적으로 나타나는 반면 남반구 여름철에는 강화된 동서 순환장의 남북으로 확장된 연직 운동지점이 발달하는 것을 볼 수 있다. 북반구 여름철의 지역 남

북 순환장의 북쪽 연직 운동 지점의 경우 북서태평양 지역의 하층 고기압성 또는 저기압성 순환장과 연결되어 있다. 북반구, 남반구 여름철에 따라 다르게 나타나는 대기 반응을 설명하는데 있어서, 중동태평양 해수면 온도 편차의 세기 및 크기, 그리고 열대 태평양과 인도양에서 해수면 온도 편차의 상전이가 발생하는 시기의 차이가 중요한 요소로 작용한다. 결과적으로 대기 변수들의 격년 변동 모드는 두 계절에서 뚜렷하게 차이를 보이며 그에 따라 아시아 몬순과 호주 몬순에도 상당히 다른 영향을 미친다.

주요어: 격년 변동성, 해수면 온도 편차, CSEOF 분석, 대기 순환, 아시아-호주 몬순 강수, 계절적 차이, 열대 인도-태평양

학생번호: 2013-22971